

# RADAR IMAGING

Ian J. Tapley

Cooperative Research Centre for Landscape Environments and Mineral Exploration.  
CSIRO Exploration and Mining, Kensington, WA 6151. E-mail: ian.tapley@csiro.au

## 1. INTRODUCTION

### Radar operation

Radar remote sensing (Henderson and Lewis, 1998) provides imagery that characterizes the physical properties (morphology, roughness, dielectric properties and geometric shapes) of the terrain surface, its cover and near-surface volume. Image enhancements are particularly suited to landform analysis from which geomorphological and geological inferences can be made. Because radars provide their own illumination, observations are independent of cloud cover, light rain, smoke haze and solar illumination, thus allowing all-time observation through all seasons and in all climatic regions. An important capability of radar is the ability to select the illumination geometry, that is, the incidence and azimuth angles, to highlight structure and other diagnostic properties of the terrain.

A typical radar measures the strength and round-trip time of the microwave signals that are emitted by a radar antenna and reflected off a distant surface or object. The radar antenna alternately transmits and receives pulses at particular microwave wavelengths (in the range 1 cm to 1 m, which corresponds to a frequency range of about 300 MHz to 30 GHz) and polarizations (waves polarized in a single vertical or horizontal plane). At the Earth's surface, the energy in the radar pulse is scattered in all directions, with some reflected back toward the antenna. This backscatter returns to the radar as a weaker radar echo and is received by the antenna in a specific polarization (horizontal or vertical, not necessarily the same as the transmitted pulse). These echoes are converted to digital data and passed to a data recorder for later processing and display as an image.

In radar imagery, surface roughness is the dominant factor in determining the amplitude of the return signal. Surface roughness is a measure of the irregularity of the terrain surface (both vertical and horizontal) compared with the radar wavelength. On radar images, surfaces can be classified as smooth, slightly rough, moderately rough or very rough, relative to the radar wavelength and angle of incidence. A consequence is that a surface that appears smooth at a long radar wavelength may appear rough at a short wavelength. The level of radar backscatter indicates the tone of an image - rough targets appear bright and smooth targets dark. The mean intensity of the radar backscatter from an area of interest is usually expressed in decibels (dB). Typical values (of  $\sigma^{\circ}$ ) for natural surfaces range from +5dB for very rough surfaces to -40db for very smooth surfaces.

Other factors that influence the intensity are the transmitting frequency (wavelength), polarization of the transmitted and received signals, incidence angle between the transmitted signal and terrain surface, topographic slope and dielectrical properties of the surface and sub-surface materials.

### Radar polarimetry

Traditional imaging radar systems measure the radar backscatter using a single frequency, single polarization antenna. An example of such a system is the radar mounted on the Canadian RADARSAT satellite that transmits and receives C-band (5.56 GHz) signals in horizontal transmit-horizontal receive (HH) polarization mode. A radar system that measures the complete polarization response of every pixel in an image is called an imaging radar polarimeter. An example is the airborne AIRSAR (AIRborne Synthetic Aperture Radar) system developed by NASA-JPL (Jet Propulsion Laboratory). Knowledge of this entire scattering matrix permits the synthesis of the radar backscatter for any combination of transmit and receive polarizations, that is, HH, HV (horizontal transmit-vertical receive), VH (vertical transmit-horizontal receive) and VV (vertical transmit-vertical receive). Radar

polarimetry is, therefore, a valuable tool for identifying the dominant scattering mechanisms present in a scene and for resolving minor differences in the physical and electrical properties between surface features.

## 2. RADAR DATASETS

Information regarding radar datasets currently available from the Australian Centre of Remote Sensing is available on the web site [http://www.auslig.gov.au/acres/prod\\_ser/index.htm](http://www.auslig.gov.au/acres/prod_ser/index.htm). These include ERS-1 and ERS-2 (European Remote Sensing), JERS-1 (Japan Earth Resources Satellite) and RADARSAT datasets. The system specifications and World Wide Web Home pages for current and future spaceborne radar instruments are listed in Table 1.

**Table 1. Spaceborne radar systems.**

Parameter	ERS-1	EST-2	JERS-1	Radarsat-1	Radarsat-2	PALSAR	ENVISAT
<b>Radar band</b>	C	C	L	C	C	L	C
<b>Polarization</b>	VV	VV	HH	HH	HH,VV HV	HH or VV HV or VH	HH, VV HV
<b>Incidence angle (degree)</b>	20-26	20-26	32-38	10-60	10-60	20-55	14-45
<b>Resolution (metres)</b>	25	25	18	8-100	3-100	10-100	30
<b>Swath width (Km)</b>	100	100	76	50-500	10-527	70-250	50-400
<b>Launch date</b>	07/91	04/95	02/92	11/95	2002	8/2002	6/2001

The AIRSAR system mentioned earlier operates in two modes. In POLSAR (POLarimetric Synthetic Aperture Radar) mode this system is capable of simultaneously collecting HH-, VV-, VH- and HV-polarized data for three frequencies: C-band (5 cm wavelength); L-band (24 cm wavelength); and P-band (68 cm wavelength). The shorter wavelength C and L bands are more sensitive to small-scale variations in surface roughness that can be related to the extent of soil erosion, size of surface lag gravels and the extent of landscape truncation. L and P bands have a greater potential for geological studies of subsurface features and the terrain below a vegetation canopy. In TOPSAR (TOPographic Synthetic Aperture Radar) mode precision elevation data are generated from the phase information accompanying the C-band VV-polarization signal using a process called radar interferometry. L and P-band polarimetric data collected in TOPSAR mode are registered to the elevation data. Examples of TOPSAR datasets are described later in this chapter.

AIRSAR datasets were recorded during airborne missions in 1993, 1996 and 2000 over selected targets in Australia, Papua New Guinea, Southeast and East Asia. Information regarding these datasets and their availability is listed on the AIRSAR Homepage <http://airsar.jpl.nasa.gov/>.

ERS-1 and -2: <http://earth.esa.int/ers>

[http://www.auslig.gov.au/acres/prod\\_ser/ersdata.htm](http://www.auslig.gov.au/acres/prod_ser/ersdata.htm)

JERS1: [http://www.auslig.gov.au/acres/prod\\_ser/eojerd.htm](http://www.auslig.gov.au/acres/prod_ser/eojerd.htm) <http://www.eorc.nasda.go.jp/JERS-1>

RADARSAT: [http://www.auslig.gov.au/acres/prod\\_ser/radadata.htm](http://www.auslig.gov.au/acres/prod_ser/radadata.htm)

<http://www.ccrs.nrcan.gc.ca/ccrs/tekrd/radarsat/rsate.html>

PALSAR: [http://www.nasda.go.jp/sat/alos/index\\_e.html](http://www.nasda.go.jp/sat/alos/index_e.html)

<http://www.eorc.nasda.go.jp/ALOS/about/overview.htm>

ENVISAT: <http://envisat.esa.int>

### 3. APPLICATIONS OF RADAR IMAGERY

#### Subsurface mapping

A major benefit of imaging radar is the ability of long wavelength signals ( $\lambda > 60$  cm) to penetrate loose overburden and map subsurface structures, provided that the volumetric soil moisture is  $< 1\%$  and the soils have fine to medium textures. This is a major advantage over reflectance remote sensing. In the Great Sandy Desert of Western Australia for example, where sandplains, dunefields and shrub-steppe vegetation obscure much of the subtle topography and underlying Proterozoic sedimentary rocks, enhancements of NASA-JPL AIRSAR data have demonstrated the benefits of polarimetric radar for revealing more information about the composition of the terrain than enhancements of either SPOT-PAN or Landsat TM data (Tapley and Craig, 1995). Figure 1 compares a Landsat TM image of bands 2:4:7 (left) with a composite image of the vertical polarization response for AIRSAR bands C:L:P (right). The TM scene highlights the ubiquitous nature of the dunefields and a composite history of fireburns, whereas the radar image “sees through” much of this cover and confusion to reveal significant geological detail. Some of the more significant observations in the image include:

1. The identification of the closure of a previously unmapped syncline [Location 1];
2. Regional extensions of alignments of truncated sedimentary sequences, much of which is subsurface, within the sandplains and pronounced expression of the geometric alignment of individual stratigraphic units [Location 2]; and,
3. Morphological evidence of a complex fluvial history under a former climatic regime that permits the construction of a sequence of palaeo-environmental events that produced the landforms associated with the palaeodrainage networks [Locations 3 and 4].

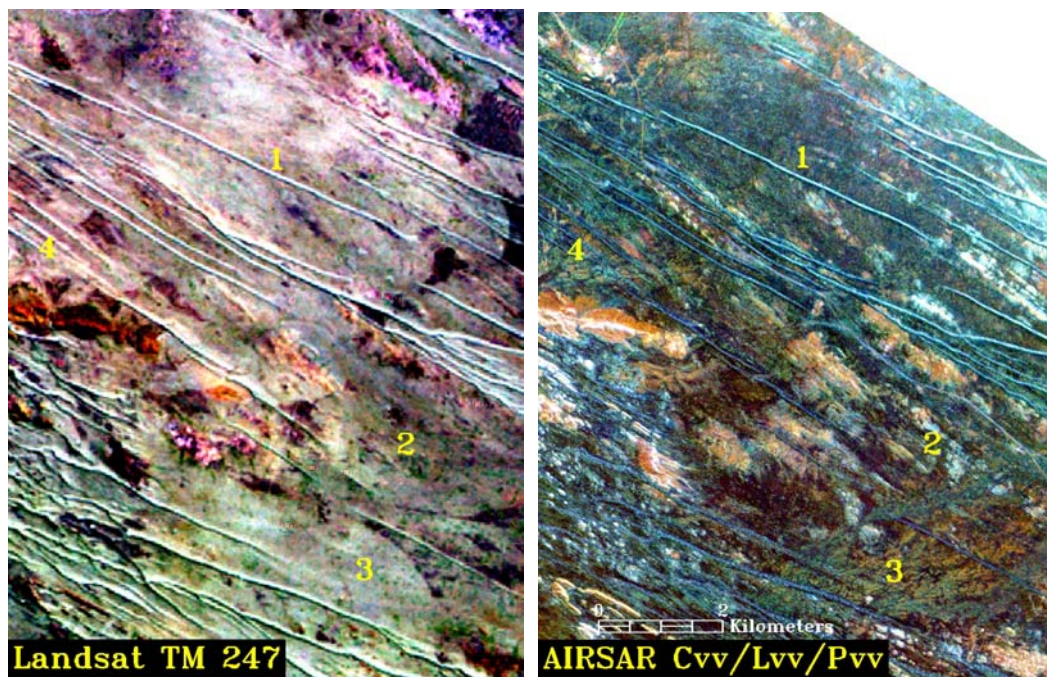


Figure 1. Images of Landsat TM and AIRSAR polarimetric data compare surface and sub-surface textural information from radar with surface mineralogy and vegetation from TM.

## Regolith and landform mapping

The benefits of radar for mapping landforms and discriminating between regolith materials in deeply weathered terrains are well described by reference to an examination of AIRSAR polarimetric data in the Gawler Craton, South Australia. Findings in the Yilgarn Craton, Western Australia, were similar (Tapley, 1998). Importantly, the fundamental attributes of a deeply weathered terrain, namely erosional and depositional regimes, can be recognized. In this topographically flat, semi-arid terrain, the most distinctive radar responses occur from prominent outcrop and associated debris of Precambrian volcanics [Figure 2, Location 1] and irregular surfaces of dissected silcrete tablelands (Location 2). These contrast strongly with a blanket of alluvial, colluvial and aeolian sediments (Location 3) with a ~10% vegetative cover of chenopod-shrubland communities, which have low-to-medium backscatter. Specific observations include:

1. The mapping of regolith-landform units is primarily a function of multi-frequency rather than multi-polarization, with the greatest sensitivity to roughness being observed in the VV-polarized data for each frequency. Regolith-landform units of the erosional regime can be delineated from those in other regimes by the increased surface roughness resulting from the accumulation of coarser lag gravels and exposure of bedrock during active erosion of the landscape. Outcrops of

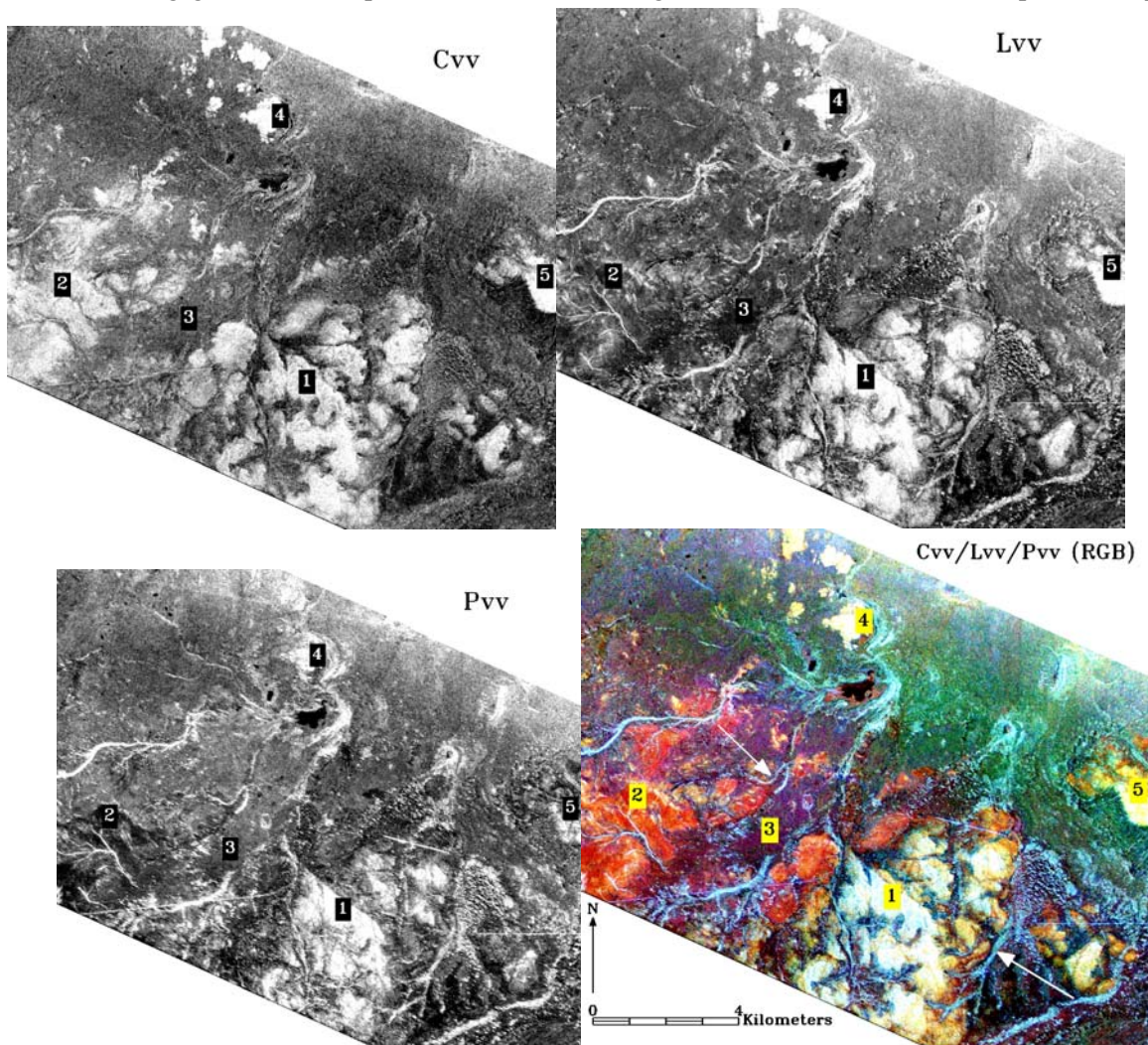


Figure 2. Variation in vertically polarized radar backscatter with changing surface roughness according to AIRSAR C, L and P band wavelengths, and a composite image of the three wavelengths. A previously unmapped NW-SE aligned linear feature [1] in the composite image is clearly evident in the Pvv band image and, to a lesser extent, in the L and C band images.

igneous rocks at Locations 1, 4 and 5 produce the strongest returns in co-polarized signals from all three frequencies and appear as white to bright yellow in the composite image.

2. Best discrimination between the landforms developed in erosional terrains is obtained from enhancements of L- and P- band data. C-band data generally do not discriminate between these landforms because their surface materials are “radar rough” at this wavelength. In Figure 2, for example, outcropping rhyodacite at Location 1 in the C-band image are confused with the medium to coarse lags of silcrete gravels and calcrete nodules developed over granite saprolite [Location 2], whereas clear distinction is made in L band. L- and, to a lesser extent, P-band signals highlight the topographic alignments of breakaway slopes that define the extent of these tablelands. Incision of the tableland by ephemeral streams has resulted in exposure and accumulations of massive to nodular calcrete and silcrete gibber that strongly backscatter the radar signals. In addition, in an area of increased dissection at Location 2, L band has clearly delineated a semi-radial pattern of isolated topographic highs of weathered granite overlain by a lag of silcrete gravels and cobbles.
3. C band provides clear discrimination between erosional and depositional terrains owing to the relative smoothness, at the scale of the L-and P-band wavelength, of regolith-landforms located in depositional terrains.

### **Terrain analysis**

An interpretation of radar images can often permit a fuller comprehension of the morphology of the landforms and the nature of the materials that form those landforms when compared with optical datasets. This interpretation is driven by a relationship between surface morphology and composition of particular landform units. For example, in the Ophthalmia Range region of the Hamersley Basin in Western Australia, a series of landscape evolution processes can be deduced from enhancements of AIRSAR imagery (Tapley, 1996). These processes were active under former climatic regimes and led to the construction of a sequence of palaeo-environmental events to produce the landforms associated with the colluvial and alluvial units. In Figure 3 two broad morphological regimes can be recognized. Extensive bedrock outcrops of the Ophthalmia Range have been, and are still part of, an erosional regime capable of supplying large volumes of material. This material has been transported and deposited in the depositional regime by both colluvial and alluvial processes to form marginal colluvial fans [Location 1], alluvial fans [Location 2] and sheetwash plains [Location 3].

The colluvial fans form a series of interconnecting, laterally coalescing, landforms. Each displays a distinctive yellow or red hue depending on the mean grain size and/or angularity of the surface lags, and the cover ratio of lag:soil:vegetation. The “yellow” fans are considered to have formed initially in the piedmont zone at the foot of the strike ridges as debris flows of locally derived coarse materials. The “red” fans are younger debris flows of slurry material formed by landslide action following deposition of the “yellow” fans. These flowed out over the “yellow” fans. During subsequent wet climatic phases, generations of alluvial fans developed as a series of discrete and topographically prominent, alluvial fan lobes over the marginal fans. Creeks since formed have developed as well-formed flow lines.

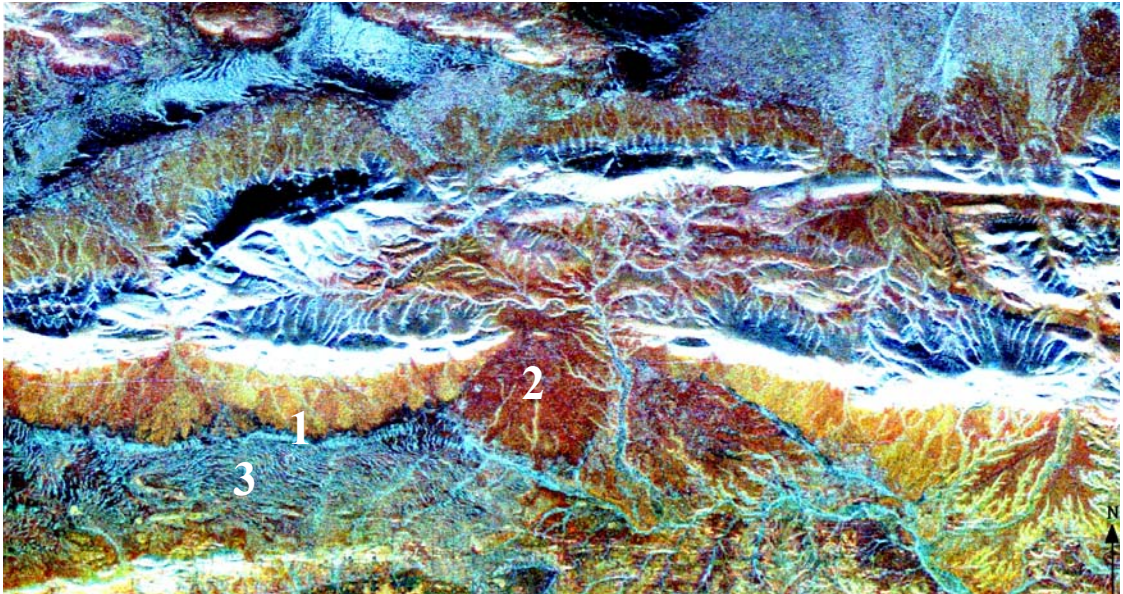


Figure 3. Landforms in vicinity of Ophthalmia Range, Hamersley Basin – a composite image of AIRSAR bands Cvv/Lvv/Pvv as RGB. Site dimensions - 16x8 km.

### Geological mapping

Enhancements of multi-parameter radar data are excellent for delineating rock units based on variations in surface roughness and dielectric properties when vegetative cover is minimal. For example, rock units within the closure of Arkaroola syncline, Flinders Ranges, South Australia, have distinct roughness properties according to their lithology, weathering and erosional characteristics. A subset of three bands Cvv/Lhv/Phv displayed as an RGB image in Figure 4 provides an accurate representation of the distribution of the rock units in the accompanying geological map. The technique is more appropriate for sedimentary sequences rather than metamorphic complexes where results have shown a poor correlation between roughness and radar backscatter (Tapley, 2000).

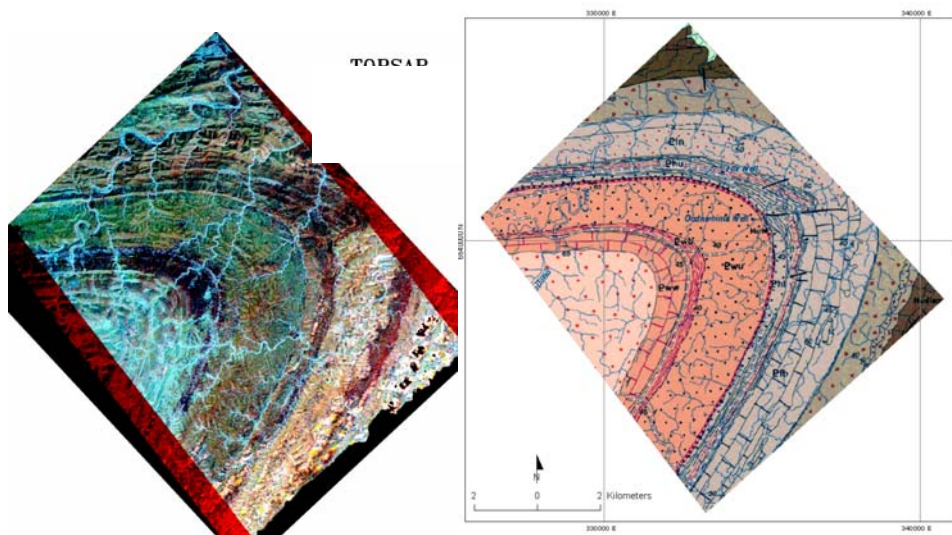


Figure 4. AIRSAR C-, L- and P-band multi-polarization composite image of stratigraphic sequence comprising Arkaroola syncline, Flinders ranges, South Australia, shows a strong relationship with the mapped geology.

Draping the radar image in Figure 4 over a precision digital elevation model would place the stratigraphic sequence in perspective with the local topography, and enhance the geological detail. Interactive viewing of 3-D perspective images on an image display screen is a simple technique for presenting the geology and landforms in a more informative way, and for understanding the relationships between landforms, geomorphic processes and terrain relief.

The highlighting and shadowing of the terrain by the side-looking illumination of radar is a distinct benefit for mapping geological structures in vegetated and non-vegetated terrains. In areas of prominent outcrop and relief, an image will commonly have a pseudo-3-dimensional perspective that highlights the position of lineaments, fault and fold structures, and morphological characteristics such as dip slopes and slope-asymmetry. For example, an enhancement of AIRSAR data in Figure 5 has provided a new insight into the geologic framework of the Ophthalmia Range region by highlighting several prominent structures within the synform, and linear extensions of these structures within the adjacent valleys (Tapley, 1996). Their appearance seems to be caused primarily by surface roughness since the alignments are mostly coincident with topographic expressions including those of stream segments, boundaries of outcrop and lithological contacts.

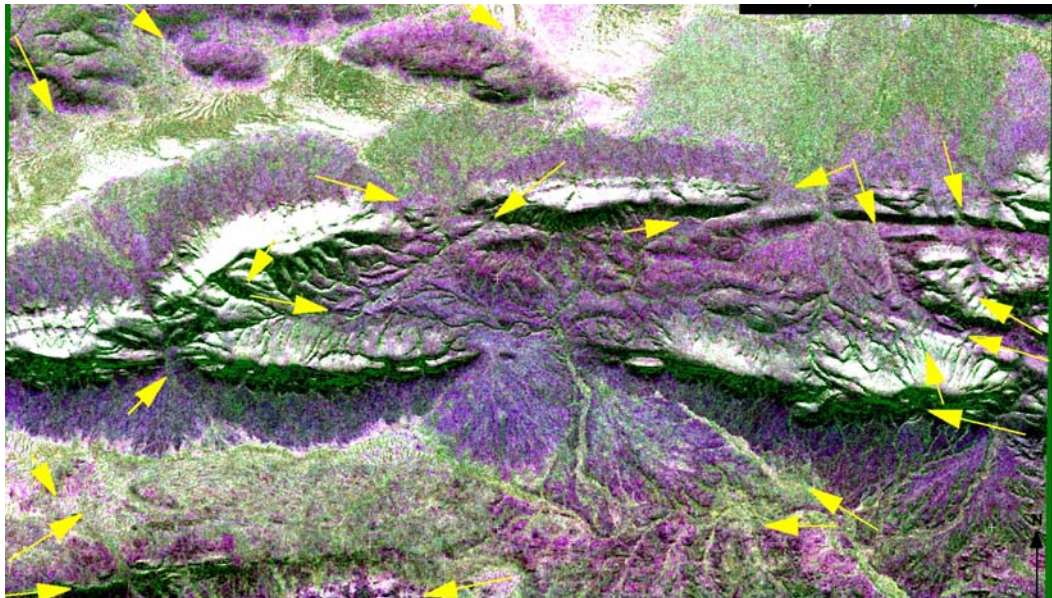


Figure 5. An interpretation of prominent linear structures from an enhancement of AIRSAR data of the Ophthalmia Range region. Site dimensions are 16x8 km, north direction to top of image.

#### 4. RADAR INTERFEROMETRY

##### Topographic mapping

Radar interferometry is an innovative technique that enables very high-resolution topographic maps of the earth's surface to be generated using spaceborne and airborne radar instruments. As with radar imagery, the technique has the advantages of automatic processing of the data, and operation in cloud, smoke and rainfall conditions, night and day. A transmit antenna mounted on a spacecraft or plane illuminates the terrain with a radar beam that is scattered by the surface. This radar echo has two components: amplitude (brightness) and phase (a measure of the distance to the target). Two receive antennas with a fixed baseline record the radar echo from slightly different positions resulting in two different radar images. The two signals received at both ends of the baseline (referred to as the interferometric baseline) show a phase shift due to differing lengths of the signal paths. The phase difference, determined by effectively subtracting the measured phase at each end of the baseline, is

sensitive to both viewing geometry and the height of the terrain. If the viewing geometry is known to sufficient accuracy, then the topography can be inferred from the phase measurement to a precision of several metres.

Interferometric data can be generated from either single-pass or repeat-pass systems. Single-pass systems such as the TOPSAR (Zebker, et al., 1992) (<http://airsar.jpl.nasa.gov/>) and Shuttle Radar Topography Mapping Mission (SRTM) instrument (<http://www.jpl.nasa.gov/srtm/>) use the two-antenna system to record both images simultaneously. Repeat-pass interferograms are generated from separate passes over the same target such as from the European ERS-1 and ERS-2 systems (<http://earth.esa.int/applications/interferometry.html>).

The height accuracy of TOPSAR digital elevation models has been shown by Madsen, et al. (1995) to be 1 m RMSE in flat terrain and 3 m in mountain areas with a 2 m RMSE overall. Typical data acquisitions are for areas of 10 km across-track and up to 60 km along track. A list of TOPSAR datasets recorded over Australia and Papua New Guinea are available on the JPL web site (<http://airsar.jpl.nasa.gov/>).

The accuracy of the data lends itself to generating precision geomorphometric and structural detail in semi-arid and humid-tropical environments. In Figure 6, shaded relief images highlight dip and strike slopes of the bedding sequence within a prominent anticline in the James Ranges, west of Alice Springs (left), and foliation trends within a metamorphic core complex masked by a canopy of tropical vegetation in Papua New Guinea (right). In the latter, it is evident that the top of the vegetation canopy conforms to the underlying topography that, in turn, is controlled by geological features and geomorphic processes. The majority of the short wavelength C-band radar backscatter is from the canopy surface thereby providing a reasonably accurate digital elevation product of the terrain.

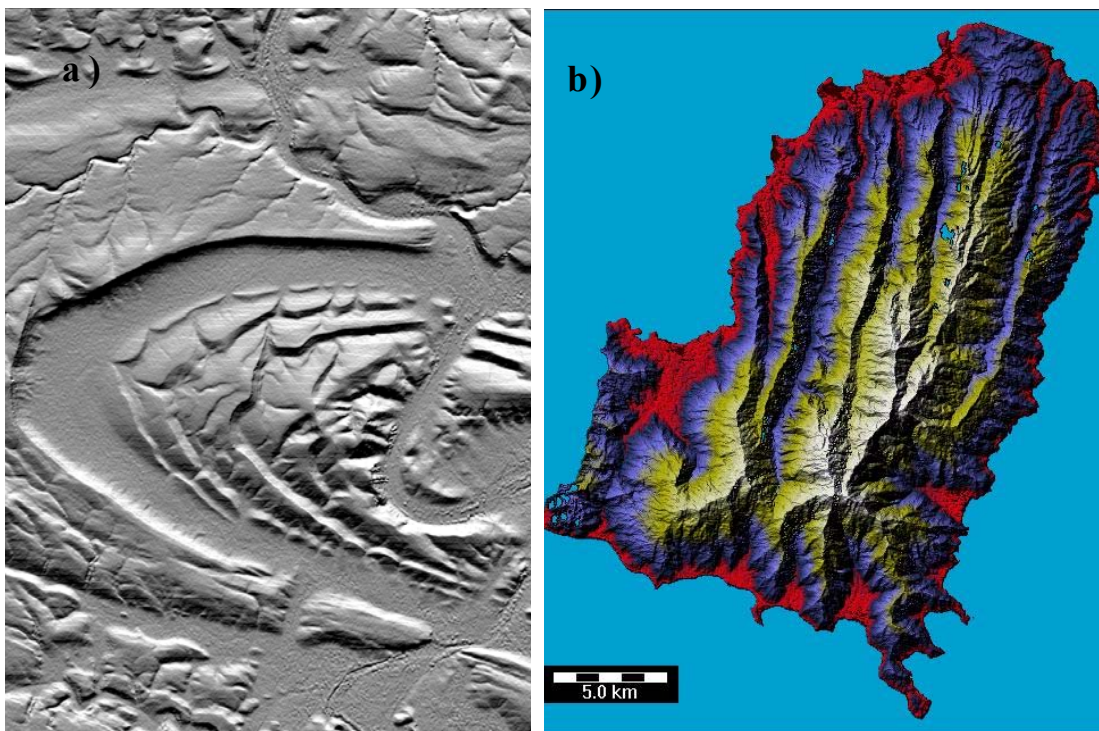


Figure 6. DEMs generated from TOPSAR radar interferometry of two contrasting terrains – semi-arid central Australia (a) and humid-tropical Papua New Guinea (b).

## Shuttle Radar Topography Mapping Mission

The Shuttle Radar Topography Mapping Mission (SRTM) in February 2000 recorded images in C-band (5.56 cm) and X band (3.1 cm) frequencies during an 11-day period. Data were acquired along 225 km wide swaths imaging Earth's entire land surface between 60° north and 56° south latitude, with data points spaced every 1 arc-second of latitude and longitude (approximately 30 m). X-band coverage occurred along narrow 50 km wide swaths and cover 40% of the area mapped by the C-band data. The absolute horizontal and vertical accuracy of the C-band data will be 30 m and 16 m, respectively. Relative height accuracy will be 10 m. However, data of these specifications will not be readily available for public use. Within 2 years, data spatially degraded to 90 x 90 m horizontal resolution but retaining the initial height accuracy, will be available at the low cost of regriding the data to a 1° x 1° area. The policy for distributing the higher resolution data is currently not clear. However, it is expected that data over politically insensitive areas, such as Australia, will be accessible. X-band DEM data of the narrower 50 km wide swath have a horizontal resolution of 30 m and relative and absolute height accuracies of 6 m and 16 m, respectively. These data will be unclassified and available for public use from the German Aerospace Centre. Both C and X-band datasets will be geometrically corrected and projected to the WGS84 datum. Extensive information describing the data products and their availability is available on the SRTM and DLR Home Pages <http://www.jpl.nasa.gov/srtm/> and <http://www.dfd.dlr.de/SRTM/november2000/html>, respectively.

## 5. USE OF RADAR DATA FOR EXPLORATION

The following recommendations are made on the use of operational imaging radar for providing detail about the morphologic and structural characteristics of most Australian terrains. As mentioned earlier, data availability is currently limited to ERS-1 and ERS-2 (C band, VV polarization), JERS-1 (L band HH polarization), Radarsat (C band HH polarization) and AIRSAR (multi-frequency polarimetric data from 1993 and 1996 PacRim1 missions). The SRTM and PacRim2 AIRSAR datasets will become available in 2001-02.

1. A combination of C (~5.5 cm), L (~24 cm) and P (~68 cm) bands is optimal for unmixing the signal response of the surface from that of the subsurface, and the ground-surface scattering from the canopy. C band has the highest priority for mapping outcropping lithologies and for discriminating between depositional and erosional terrains. L band is most sensitive to scales of surface change that occur through erosion of the regimes, and P band is preferred for mapping subsurface structures. However, because of distortions to low-frequency signals beyond the earth's atmosphere, P band can operate effectively only from an airborne system. Therefore L band is currently the longest wavelength possible in a spaceborne system. Increased penetration of both soil and vegetation cover can be obtained from an airborne ultra-wide-band radar system operating with wavelengths >100 cm provided that soil moisture and green biomass levels are minimal.
2. VV and HV (or VH) are the polarizations of choice for geological mapping in arid/semi-arid lands. Although VV and HH polarizations both result in useful SAR images for the majority of the terrains, VV is favoured because of its increased sharpness and ability to provide better discrimination between surfaces having similar roughness characteristics. The HV (VH) polarization for P band provides the best indication of volume scattering from the shallow subsurface. In woodland terrains, HH-polarization signals suffer less attenuation from the vertically aligned tree trunks and are more likely to provide information about the physical characteristics of the underlying ground-surface. The cross-polarized HV scattering coefficients are less dependent on incidence angle than the co-polarized (HH and VV) scattering coefficients. They are also less sensitive to variations in terrain slope. If geobotanical relationships exist or are being sought, VV-polarization data are preferred since they have increased interaction with the tree trunks.
3. A spatial resolution of approximately 10 m is necessary to resolve many of the narrow alignments of subcrop and lithic fragments found in sandy arid terrains. For general synoptic mapping and morphologic characterization, a footprint of 20 m will probably suffice.

4. Incidence angles of between 30° and 50° are recommended for mapping surficial bedrock units and regolith materials based on variations in their surface roughness. Angles <30° can reduce the ability of the radar signals to discriminate between surfaces of different RMS roughness levels, although in sandy terrains, the steep 23 degree angle of incidence of ERS data is a distinct advantage since the majority of outcrop is low profile and intermittent.
5. For maximum geological information, the flight direction should parallel the regional strike, or be within 45° of strike if there are several suites of geological structures present. In sand-ridge terrain, if there is no preferred direction, the flight lines are best positioned orthogonal to the dune direction. The current spaceborne radar sensors including those on the Radarsat, ERS-1 and JERS satellites collect data from ascending and descending passes meaning that both east-looking and west-looking azimuth directions are available.

## **6. PROCESSING AND LIMITATIONS OF RADAR DATASETS**

Such is the high level of radiometric quality of AIRSAR data that enhancements derived from these data can be used in their original form for valid interpretations. Nevertheless, it is widely recognized that radar datasets collected from airborne platforms do regularly contain an unwanted signal component, commonly referred to as “noise” introduced by system and aircraft electronics. In addition, all radar datasets contain an inherent random and multiplicative “noise” component called “speckle” that has the capability to reduce the visual information content of the data, especially in the shorter wavelength bands. Much of this is due to the coherent nature of the return signals.

A technique used regularly to reduce speckle in spaceborne and airborne datasets has been that of spatial filters. A common finding from examinations of speckle filters is the superiority of adaptive filters, such as Lee and Frost filters, over the standard digital noise filters such as low pass and median filters. Ideally, a filter should reduce speckle while preserving the radiometric information (the radar backscatter value), and the spatial sharpness in the data. Adaptive filters essentially retain important high-frequency detail in the form of point of small targets whereas the standard convolutions filter, for example the median filter, smoothes the data obliterating narrow linear features. However, experience with processing ERS and JERS datasets of sandplain regions has demonstrated the benefit of a 3 x 3 median filter for suppressing much of the scene speckle. Speckle and “noise” reduction can also be achieved in the ENVI image processing software <http://www.rsinc.com/envi/> by implementing the Minimum Noise Fraction (MNF) Rotation option. Advice on its proper use should be sought from the author.

Enhancements of ERS-1, JERS-1 or RADARSAT datasets cannot resolve the detailed information about the land-surface observed in images of equivalent AIRSAR wavelength-polarization band combinations. Maximum value for each can be gained from the synoptic view afforded by small-scale images and image mosaics of large areas. This is especially applicable to JERS data, where the degrading effects of speckle and reduced radiometric integrity are visually concealed by the scale of the data.

Designed for ocean observations, the ERS radar instruments are not ideally configured for geological applications. Over hilly terrains, the steep incidence angle will promote topographic distortion in the data. However, in low-relief terrains, the steep incidence angle has the potential to provide maximum discrimination between outcrop and non-outcrop, and to differentiate between lithologies featuring surfaces with different and near-similar erosional characteristics. In sand-ridge terrains, where the radar signal responds strictly to the physical characteristics of the surface elements, the synoptic view can “piece-together” scattered outcrop into sensible alignments and patterns to allow an improved synthesis of the regional, geological picture.

Unfortunately the authors experience of RADARSAT data has been limited to two scenes of Fine-1 Near Beam mode data – one in prominent sedimentary outcrop with minimal vegetation, another in low relief, degraded terrain with a regular cover of chenopod shrubs. Both scenes were severely

contaminated by speckle that required vigorous spatial filtering to suppress. Once filtered, the resultant images contained less information than are available from optical datasets, including aerial photographs.

Experience with AIRSAR data of degraded landscapes has shown that colour-composite images of AIRSAR data, processed to remove geometric and radiometric errors, will generally permit the recognition of the principal and subtle attributes of the terrain when the multi-frequency bands are ideally assigned to the colour components of an RGB display. However, felsic erosional landforms such as stripped convex hills, are seldom discernible from equivalent units in mafic terrain owing to similar radar responses from the surficial regolith materials of these landforms. Their separation can be best achieved from mineralogical differences observed on enhancements of Landsat TM data. In subtropical woodlands, images of AIRSAR data are very useful for recognizing the structural fabric of a region, but they cannot resolve landforms with the same definition as 1:25 000-scale aerial photographs.

The processing of polarimetric radar data requires the use of specialized tools included in commercial image-processing software packages such as ENVI (<http://www.rsinc.com/envi/>) and RADARSOFT ([http://www.pcigeomatics.com/product\\_ind/easipace.html](http://www.pcigeomatics.com/product_ind/easipace.html)). Most packages have the adaptive filters necessary to process the single-band datasets.

## REFERENCES

- Henderson, F.M. and Lewis, A.J., 1998. Principles and applications of imaging radar. Manual of Remote Sensing, 3<sup>rd</sup> Edition, Volume 2. American Society for Photogrammetry and Remote Sensing. John Wiley & Sons Inc, Canada 866 pp.
- Madsen, S. N., Martin, J.M. and Zebker, H.A., 1995. Analysis and evaluation of the NASA/JPL Across-Track Interferometric SAR System. Institute of Electrical and Electronic Engineers (IEEE) Transactions on Geoscience and Remote Sensing 33(2): 383-391.
- Tapley, I.J. and Craig, M.D., 1995. An evaluation of AIRborne Synthetic Aperture Radar (AIRSAR) for mapping surface and sub-surface structures in the Telfer region, Paterson Province, Western Australia (Volumes 1 and 2). CSIRO/AMIRA Project 392. CSIRO Exploration and Mining Report 146R, pp. 110.
- Tapley, I.J. 1996. An assessment of airborne synthetic radar (AIRSAR) as an aid to iron exploration in the Hamersley Basin, Western Australia. Executive summary report. CRC LEME Restricted Report 12R. CSIRO Exploration and Mining Report 282R. pp. 15.
- Tapley, I.J., 1998. Landform, regolith and geological mapping in Australia using polarimetric and interferometric radar datasets – Executive Summary Report. CRC LEME/AMIRA Project 392. CRC LEME Report 90R. CSIRO Exploration and Mining Report 529R. pp. 38.
- Tapley, I.J., 2000. Geological mapping and terrain analysis in Australia using multifrequency, polarimetric radar data. The recognition of geological units within the Flinders and Olary Ranges, South Australia (Volumes 1 and 2). Prepared for Sumitomo Metal Mining Co. Ltd. CRC LEME Restricted Report 154. pp. 93.
- Zebker, H.A., Madsen, S.N., Martin, J., Wheeler, K.B., Miller, T., Lou, Y., Alberti, G., Vetrella, S. and Cucci, A., 1992. The TOPSAR interferometric radar topographic mapping instrument. Institute of Electrical and Electronic Engineers (IEEE) Transactions on Geoscience and Remote Sensing 30(5): 933-940.